

Using Inverse Design Method to Investigate the Objective Focal Properties for Asymmetrical Magnetic Field

Abdoun K. Al-Saady

Department of Physics , College of Science , Karbala University Mohammed J. Yassen

Saadi R. Abas

Khalid H. Abd

Department of Physics , College of Education , Al-Mustansiriyah University

Abstract

In this research depending on inverse design method to investigate the objective focal properties for asymmetrical magnetic field by using the axial distribution of the magnetic field for (Grivet-Lenz model) . The influence of the magnetic field model parameters on the objective focal properties and the pole pieces profile of asymmetrical magnetic electron lenses has been taken into account .

The results have shown that the most effective parameters on the design configuration are the two half widths of the axial magnetic field distribution .Also , the pole pieces of various asymmetrical double pole piece magnetic lenses can be reconstructed according to the different half widths of the field on the object and image sides .

الخلاصة

اعتمد هذا البحث طريقة التصميم العكسي في دراسة الخواص البؤرية الشبكية لمجال مغناطيسي لامتناظر بالاستعانة بالتوزيع المحوري للمجال المغناطيسي لأنموذج - كرفت لنز . لقد اخذ بنظر الاعتبار تأثير معلمات النموذج المستخدم على الخواص البؤرية الشبكية والمظهر الجانبي لأقطاب العدسات المغناطيسية اللامتناظرة .

أظهرت النتائج إن المعاملات الأكثر تأثيراً على شكل التصميم تتمثل بعرضي النصف لتوزيع المجال المغناطيسي المحوري كذلك إن أقطاب العدسات المغناطيسية ثنائية القطب اللامتناظرة المتنوعة يمكن إعادة تركيبها حسب عرض النصف المختلف للمجال على جانبي الجسم والصورة .

1.Introduction

The synthesis technique is considered to be on the best method for improving the work or performance of the magnetic lenses and its saves time in comparison with the analytical procedure which takes much more time. In this research an analytical function has been used (Grivet-Lenz model) for representing the axial magnetic scalar potential distribution through which its asymmetrical axial magnetic field distribution has been reached and its objective focal properties such as (spherical and chromatic aberration coefficients and focal length) at two sides of asymmetrical axial magnetic field distribution and then comparison between them under zero and infinite magnification conditions .

Depending on the similarity between the curve shapes of the axial magnetic field distribution and the hyperbolic tangent function, this function has been used for representing the electron beam trajectory r_z as shown by the following form [Szilagy, 1988]:

$$r_z = \alpha \tanh \left(\frac{z}{\beta} \right) \quad z_S \leq z \leq z_E \quad (1)$$

where z_S and z_E are the initial and final axial coordinates of the optical axis and $(\alpha = w \cdot B_{\max} / 2\mu_0)$, $(\beta = w / 2)$, where μ_0 is the space permeability and equal $4\pi \times 10^{-7} \text{ H.m}^{-1}$, w is the half width and B_{\max} is the maximum magnetic flux density.

Since the magnetic lens is symmetrical, the magnetic field also is symmetrical, thus $|z_S| = z_E$, therefore the lens length $L=2|z_S|$ or $L=2z_E$ or another word $B_z(z)=B_z(-z)$. Hence the lens length L is put as optimization parameter in above mentioned of the two parameters w and B_{\max} . The calculation of the magnetic flux density distribution along the optical axis has been calculate from the following paraxial ray equation [Juma and Mulvey, 1974; Zhigarev, 1975; Juma and Mulvy, 1978]:

$$r'' + \frac{\eta}{8V_r} B_z^2 r = 0 \quad (2)$$

where r'' is the second derivative of the electron beam trajectory, r is the electron beam trajectory, η is the charge -to- mass quotient of the electron, V_r is the relativistically-corrected accelerating voltage and B_z is the axial magnetic flux density distribution along the optical axis. Then we can re-write the equation (2):

$$B_z^2 = - \left(\frac{8V_r}{\eta} \right) \left(\frac{r''}{r} \right) \quad (3)$$

Now by derivative the equation (1) twice we get:

$$r' = \left(\frac{\alpha}{\beta} \right) \sec h^2 \left(\frac{z}{\beta} \right) \quad (4)$$

$$r'' = - \left(\frac{2\alpha}{\beta^2} \right) \sec h^2 \left(\frac{z}{\beta} \right) \tanh \left(\frac{z}{\beta} \right) \quad (5)$$

From substitution the equation (5) in the equation (3) we get :

$$B_z^2 = - \left(\frac{8V_r}{\eta} \right) \left(\frac{- \left(\frac{2\alpha}{\beta^2} \right) \sec h^2 \left(\frac{z}{\beta} \right) \tanh \left(\frac{z}{\beta} \right)}{\alpha \tanh \left(\frac{z}{\beta} \right)} \right) \quad (6)$$

This equation led to:

$$B_z = \left(\frac{16V_r}{\eta\beta^2} \right)^{1/2} \left[\sec h \left(\frac{z}{\beta} \right) \right] \quad (7)$$

Suppose the relations as shown by the following forms:

$$B_{\max} = \left(\frac{16V_r}{\eta\beta^2} \right)^{1/2} \quad (8)$$

$$z = \frac{w}{2} \quad (9)$$

$$B_z \left(\frac{w}{2} \right) = \frac{1}{2} B_{\max} \quad (10)$$

Put the equations (8), (9) and (10) in the equation (7) we get :

$$\frac{1}{2} B_{\max} = B_{\max} \operatorname{sech} \left[\frac{w}{2\beta} \right] \quad (11)$$

$$\frac{1}{2} = \operatorname{sech} \left(\frac{w}{2\beta} \right) = \frac{1}{\cosh \left(\frac{w}{2\beta} \right)} \quad (12)$$

$$\cosh \left(\frac{w}{2\beta} \right) = 2 \quad (13)$$

$$\left(\frac{w}{2\beta} \right) = \operatorname{arccosh} (2) = 1.317 \quad (14)$$

$$\beta = \left(\frac{w}{2.634} \right) \quad (15)$$

$$B_z = \frac{B_{\max}}{\cosh \left(\frac{2.634 z}{w} \right)} \quad (16)$$

The relationship between the half width and the half half width is ($w=2a$), then equation (16) becomes:

$$B_z = \frac{B_{\max}}{\cosh \left(\frac{1.317 z}{a} \right)} \quad (17)$$

where B_z is the axial magnetic flux density distribution along the optical axis z , B_{\max} the maximum magnetic flux density and a the half half width of the magnetic field. It can be seen that equation (17) representing the (Grivet-Lenz model) and has three main control parameters that B_{\max} , a and z . In the present research the parameter has been studied only a and other two parameters were kept constant ($B_{\max}=1\text{T}$ and $L=40\text{mm}$).

2.Field Distribution

The axial magnetic flux density distribution B_z along the optical axis z may be represented by the following well-known field model(Grivet-Lenz model) equation (17). The half width is the axial distance from the position of maximum field B_{\max} to the point where the field has fallen to half this value. In the present work various asymmetrical field distributions have been taken into account. The maximum flux density (B_{\max}) is considered to be located at $z=0$; it is a point of inflection of the magnetic field and the zero coordinate of the optical axis divides the asymmetrical field into two unequal parts.

It should be mentioned that in a symmetrical magnetic lenses B_{\max} is situated at the centre of the air gap separating the two pole pieces. However, in asymmetrical lenses B_{\max} is situated in the vicinity of the smaller bore pole piece. In terms of coordinates B_{\max} may be located at a point on the optical axis other than zero.

Equation (17) is applied to compute the asymmetrical axial flux density distribution B_z for the two unequal regions about the zero coordinate. In the present work the field asymmetry is obtained by varying the various parameters of the axial field such as its half width and its axial extension. The denominator of equation (17) is $[\cosh(1.317(-z/a_1))]$ for the half width a_1 on negative z and it is $[\cosh(1.317(z/a_2))]$ for the half width a_2 on positive z .

The total half width a of the asymmetrical axial field is the sum of the two half widths a_1 and a_2 , i.e. $a=a_1+a_2$. When $a_1=a_2$ the axial flux density distribution will be symmetrical whereas if $a_1 \neq a_2$ the distribution will be asymmetrical. In an asymmetrical objective lens, one part of the axial field acts as a condenser and the other part acts as an objective. The function of each part of the axial field depends on the direction of entry of the electron beam.

Figure (1) shows a diagram of an asymmetrical axial magnetic field where B_{\max} is located at $z=0$. The object side field extends along negative z and has a half width a_1 whereas the image side field is along positive z and its half width is a_2 . It is assumed to a good of accuracy that the axial extension of the field along the z -axis is represented by the distance L . The field at distances greater than L is neglected since its effect in practice is insignificant. The area under the curve of the axial asymmetrical flux density distribution is computed by using Ampere's law [Grivet, 1972; Hawkes and Kasper, 1989]:

$$\int_{Z_B}^{Z_E} B_z dz = \mu_o NI = \mu_o (V_1 - V_2) \quad (18)$$

where NI is the excitation of the magnetic lens in ampere-turns, and V_1 and V_2 are the magnetic scalar potentials on the two ends of L .

Computations on the two parts of the asymmetrical field have been carried out under various conditions. By keeping B_{\max} , a_2 and L constants, the object side field has been computed at various values of a_1 . Similarly, the image side field has been computed at various values of a_2 by keeping B_{\max} , a_1 , and L constants and also the effect of L on the focal properties has been investigated.

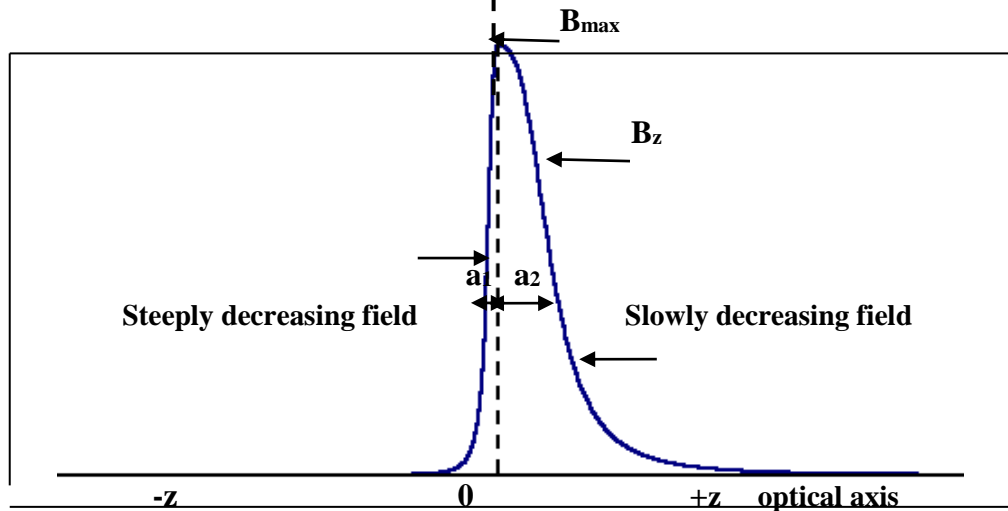


Figure (1): Asymmetrical axial field distribution of a double pole piece magnetic lens .

3.Pole piece Reconstruction

To determine the lens potential, the region of its axial extension is divided into (n-1) subintervals where n represents the points of the field along the z-axis. By numerical analysis the axial magnetic flux density distribution B_z is represented by a cubic spline function in each subinterval as shown in the following equation [Al-Obaidi, 1995]:

$$B_z = -\mu_o \frac{dV_z}{dz} \quad (19)$$

and with the aid of the cubic spline technique, the axial magnetic scalar potential may be given by:

$$V_{Z(k+1)} = V_{Zk} - G_k \quad (20)$$

where:

$$G_k = \mu_o^{-1} \left[B_k h_k + B'_k \left(\frac{h_k}{2} \right)^2 + B''_k \left(\frac{h_k}{2} \right)^3 + \left(\frac{B''_{k+1}}{3} \right) \left(\frac{h_k}{2} \right)^3 \right]$$

Here $h_k = z_{k+1} - z_k$; it represents the width of each subinterval. When the lens is symmetrical $V_{Z(n)} = -V_{Z(1)} = 0.5 \text{ NI}$.

Consider the magnetic field model given in equation (17) is determined under asymmetrical conditions along the optical axis. Since the lens is asymmetrical, then the absolute value of the potentials at the lens terminals are not equal in magnitude (see figure 2). This indicates that the area under the condenser and objective fields are not equal. At the plane where $z=0$ the potential is zero as shown in figure (2). The lens asymmetry is achieved by maintaining this plane and keeping the condenser field on its left-hand side and the objective field on the right-hand side. Equation (20) is applied on each of the two above-mentioned fields since these two fields are not identical.

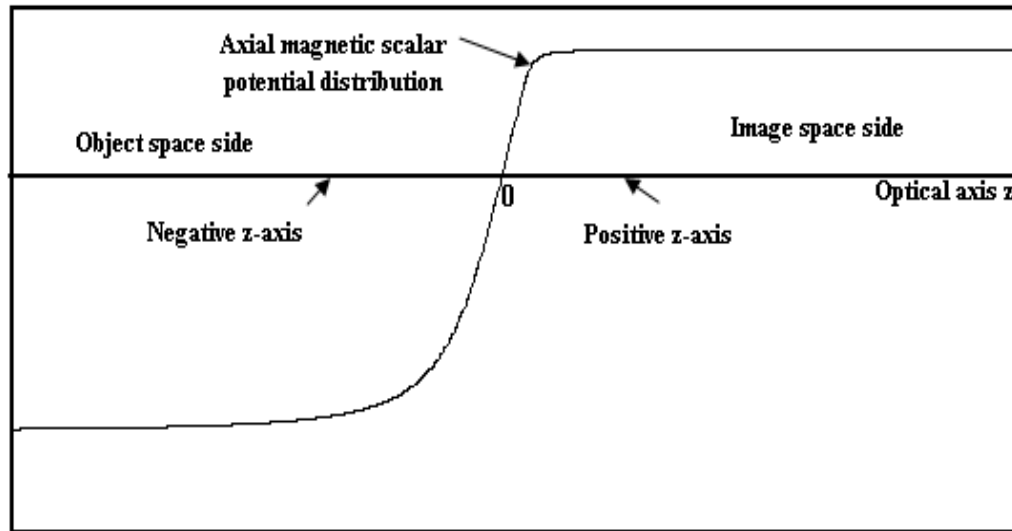


Figure (2) :Potential distribution of asymmetrical double pole piece magnetic lens.

4. Results and Discussion

The maximum flux density B_{max} , the two half widths of the asymmetrical field on the object and image sides a_1 and a_2 respectively, and the axial length of the field have been taken into consideration as optimization parameters for the asymmetrical lens. The objective focal properties of each lens of specific asymmetry parameters have been investigated under zero and infinite magnification conditions. In the former the electron beam enters the lens field parallel to the optical axis and emerges after crossing the axis once whereas in the latter the beam is on the axis before it enters the lens and emerges parallel to the optical axis. The electron beam experiences two different magnetic fields *in the region of B_{max} i.e. about the zero coordinate on the optical axis*. The lenses are investigated in the absence of magnetic saturation where the flux density $B(r, NI)$ generated by a coil of excitation NI ampere-turns is proportional to NI [Hawkes, 1982; Al-Saadi, 2007] :

$$\frac{\partial B(r, NI)}{\partial (NI)} = \frac{B(r, NI)}{(NI)} \quad (21)$$

The linearity of equation (21) holds if the flux density within the pole pieces and shielding material is sufficiently low, and if the magnetic permeability is sufficiently high. The magnetic field strength H within the material may be neglected and the magnetic scalar potential is defined by the following equation:

$$H(r) = -\text{grad } V(r) \quad (22)$$

When the magnetic lens is symmetrical about the mid-plane the absolute value of the magnetic scalar potential on the object side is equal to that on the image side i.e., the electron beam suffers the same refractive power on both sides of the magnetic field. However, in the case of asymmetrical double pole piece lens these two values are not equal to each other since the magnetic scalar potential on the object or image side would be greater or less than the other depending on the number of ampere-turns under the condenser and objective fields. The sum of the absolute values of the magnetic scalar potentials on the object and image side is equal to the total excitation of the lens according to Ampere's law (see equation 18).

Figure (3) shows the axial magnetic field distribution B_z for different values of the half width a_1 ($a_1=1, 2, 3, 4, 5\text{mm}$) on the object side by maintaining $B_{\max}=1\text{T}$, $a_2=1\text{mm}$ and $L=40\text{mm}$. It should be noted that the distribution of the field on the image side is not affected since a_2 is kept constant. The total number of ampere-turns as well as the number of ampere-turns under the condenser field increase with increasing a_1 . This means that the absolute value of the magnetic scalar potential on the object side increases with increasing a_1 as shown in figure (4).

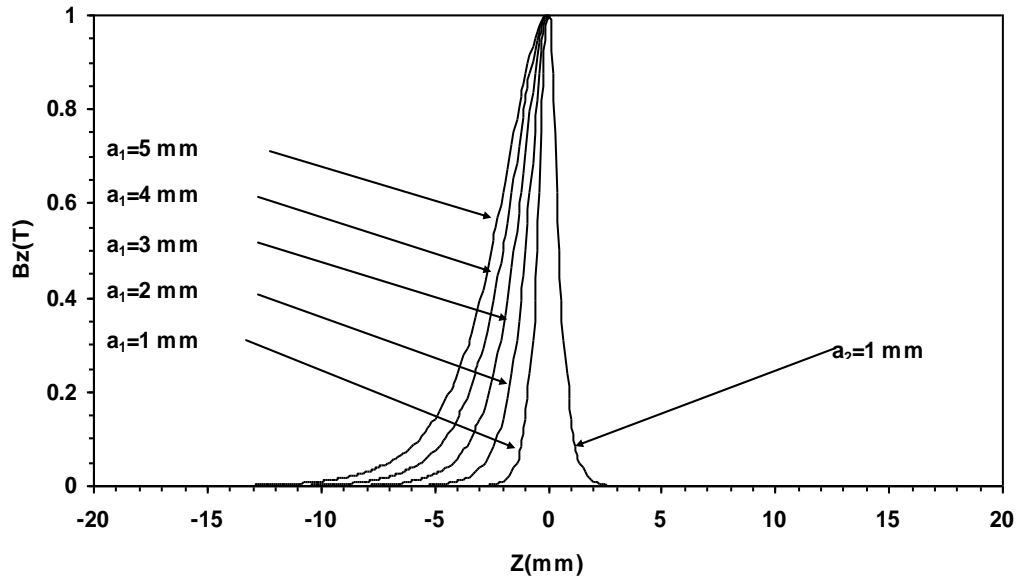


Figure (3): The axial magnetic field distribution for different values of a_1 ($a_1=1, 2, 3, 4, 5\text{mm}$) when $B_{\max}=1\text{T}$, $a_2=1\text{mm}$, and $L=40\text{mm}$.

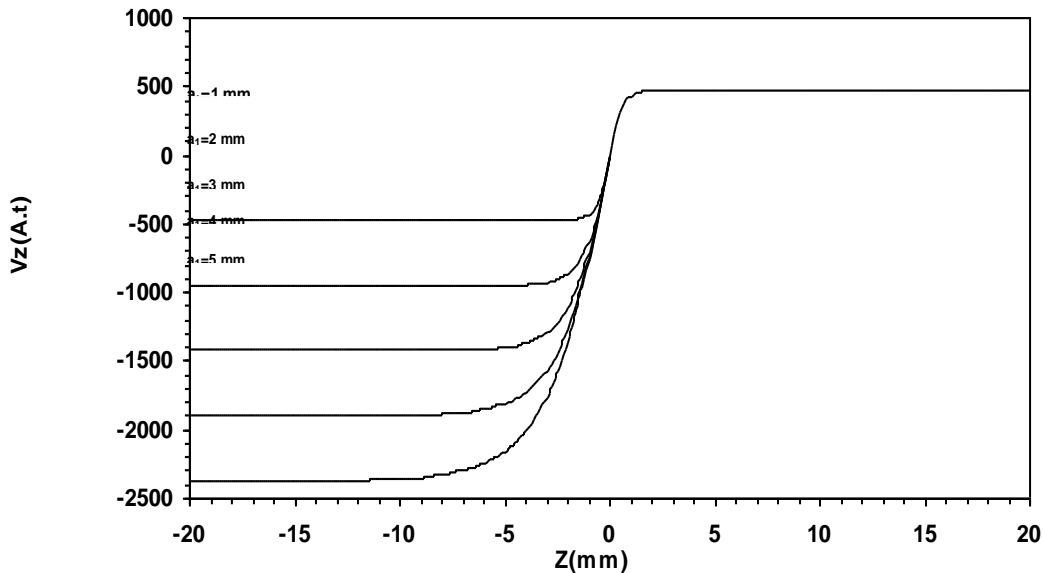


Figure (4): The axial magnetic scalar potential distribution for different values of a_1 ($a_1=1, 2, 3, 4, 5\text{mm}$) when $B_{\max}=1\text{T}$, $a_2=1\text{mm}$, and $L=40\text{mm}$.

By using the reconstruction procedure of the magnetic lens pole pieces, figure (5) shows the upper half of the pole piece for various values of a_1 when the other optimization parameters are kept constants. It should be mentioned that when $a_1=a_2=1\text{mm}$ the resulting

lens is symmetrical; however, for the other values of a_1 the magnetic lens becomes asymmetrical with different bore diameters about the mid-plane and the distance between the two faces of the pole pieces increases with a_1 [Al-Batat et al , 2005].

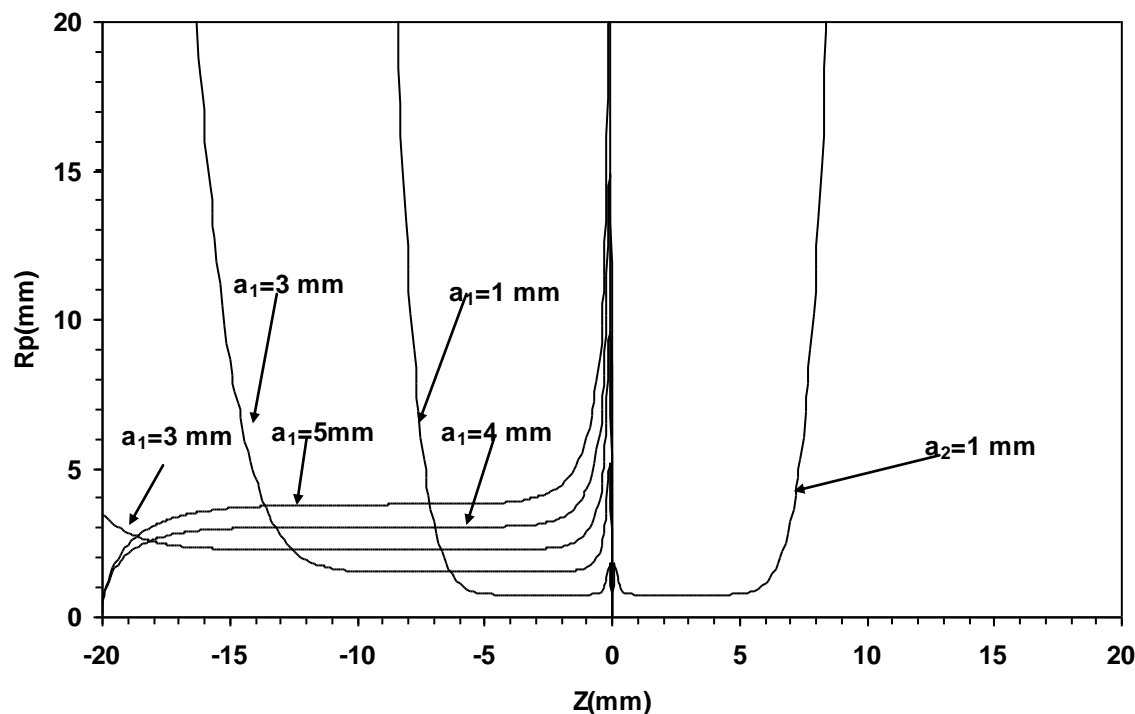
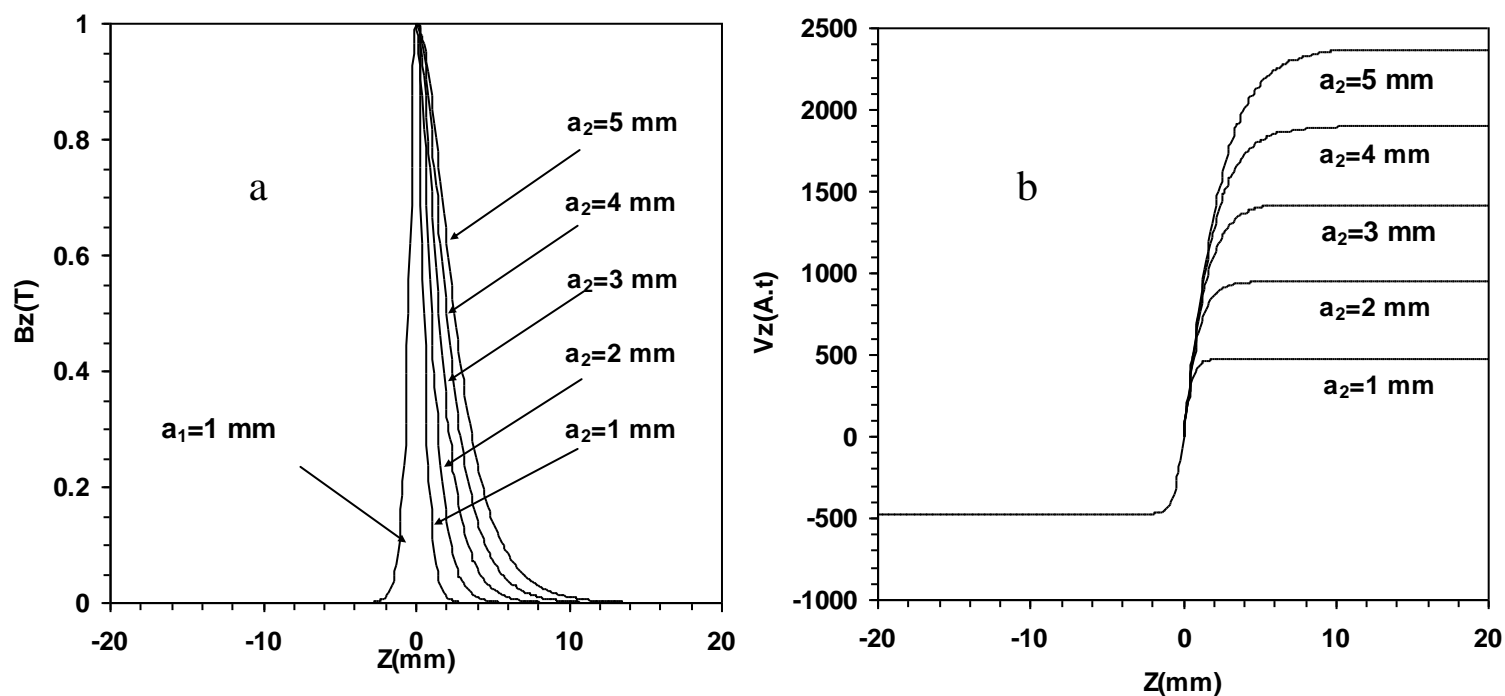


Figure (5): Profile of pole pieces for different values of a_1 ($a_1=1, 2, 3, 4, 5$ mm) when $B_{\max}=1$ T, $a_2=1$ mm, and $L=40$ mm.

The half width a_2 on the image side space is now given the same values as those on the object side space a_1 in the mathematical model for calculating the axial magnetic field i.e. $a_2=1, 2, 3, 4, 5$ mm as shown in figure (6a). The other parameters remain the same as those used in calculating the axial magnetic field for different values of a_1 i.e. $a_1=1$ mm, $B_{\max}=1$ T, and $L=40$ mm. It is found that the distributions of the axial magnetic field and its axial magnetic scalar potential distribution for different values of a_2 are the same as those for a_1 , but the left side becomes right and the right side becomes left as shown in figure (6b). This result means was found the corresponding of pole piece profile for different values of a_2 as shown in figure (7). Variation of the lens excitation NI in ampere-turns with each of the two half widths a_1 or a_2 as shown in figure (8). It indicates that in order to increase the width of a_1 or a_2 one should increase the lens excitation NI .



Figure(6): (a)The axial magnetic field distribution and (b)the axial magnetic scalar potential distribution for different values of a_2 ($a_2=1, 2, 3, 4$, when $B_{max}=1T$, $a_1=1mm$, and $L=40mm$).

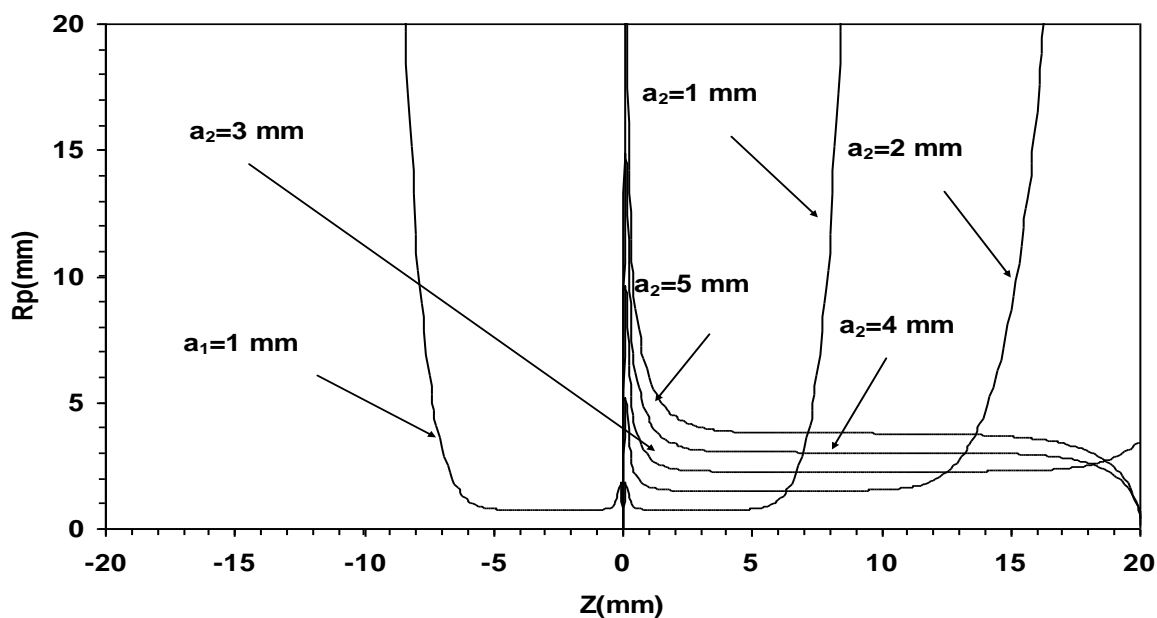


Figure (7): Profile of pole pieces for different values of a_2 ($a_2=1, 2, 3, 4, 5mm$) when $B_{max}=1T$, $a_1=1mm$, and $L=40mm$.

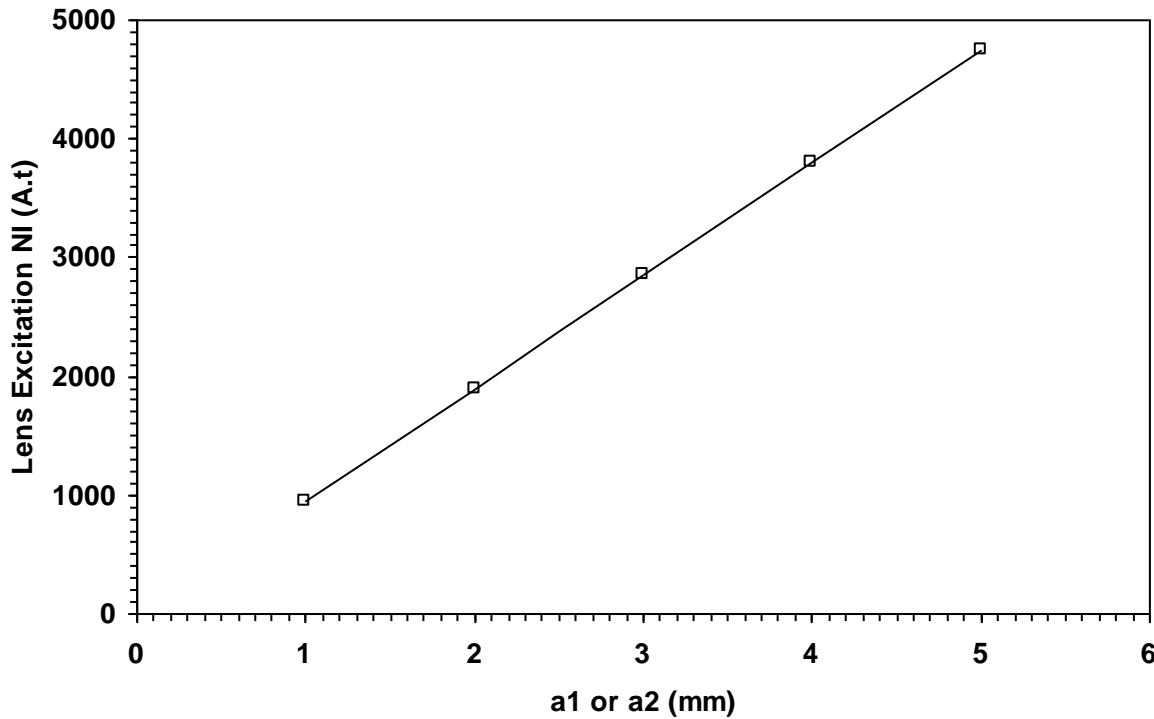


Figure (8): Variation of the lens excitation NI with the half widths a_1 and a_2 .

Variation of the objective focal length f_o , spherical aberration coefficient C_s , and chromatic aberration coefficient C_c with the object space side half width a_1 and image space side half width a_2 at the excitation parameter $NI / V_r^{1/2} = 30$ for zero and infinite magnification conditions as shown in figure (9). It should be noted that the objective properties under zero magnification condition for different values of a_1 are equal to those under infinite magnification condition for the same values of a_2 on the image side. Also these properties under infinite magnification condition for different values of a_1 are equal to those under zero magnification condition for the same values of a_2 on the image side.

For asymmetrical axial magnetic field of different values of a_1 and a_2 , it is noted that the maximum value of the flux density B_{\max} has no effect on the objective focal properties and the pole piece profile since the total half width is kept constant. Furthermore, there is no effect of the asymmetrical lens length on the focal properties and the pole piece profile when the lens length is changed by equal values on its two sides [Al-Batat *et al* , 2005].

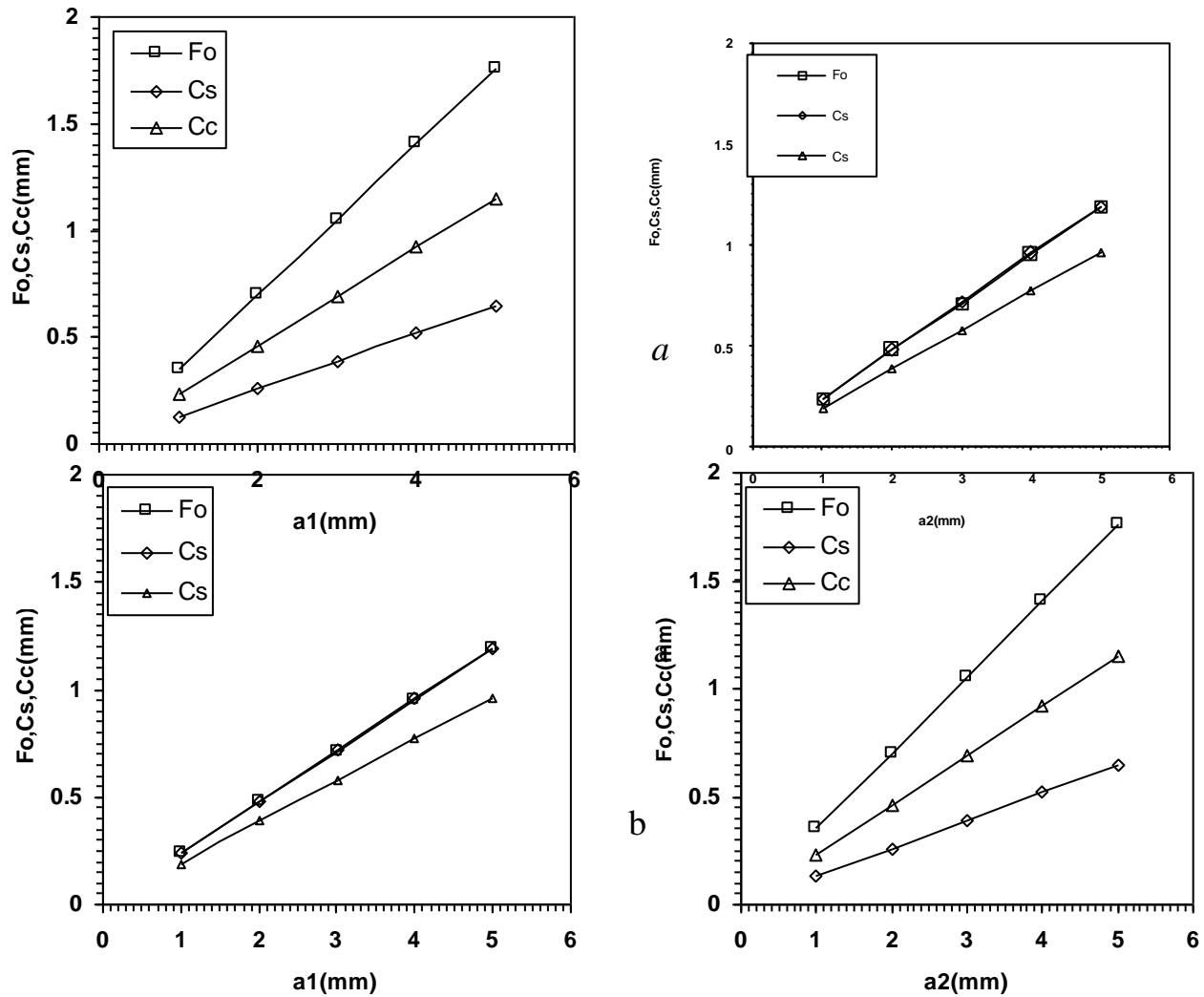


Figure (9): The objective focal length f_o , the spherical aberration coefficient C_s , and the chromatic aberration coefficient C_c against the object space side half width a_1 and the image side half width a_2 when $B_{max}=1T$, and $L=40mm$:

(a) zero magnification condition ; (b) infinite magnification condition.

In tables (1) and (2) it was found that the values of the relative spherical and chromatic aberration coefficients C_s/f_o and C_c/f_o respectively are quite favorable in high resolution electron microscopes since they are less than unity at various values of a_1 . This result indicates that the performance of such asymmetrical objective lenses is desirable in the field of electron microscopy [Al-Batat *et al* , 2005].

Table (1): The objective focal properties for different values of a_1 under zero magnification condition at $NI / V_r^{1/2} = 30$.

a_1 mm	f_o mm	C_s mm	C_c mm	C_s/f_o	C_c/f_o
1	0.35	0.13	0.23	0.37	0.66
2	0.70	0.26	0.46	0.37	0.66
3	1.05	0.39	0.69	0.37	0.66
4	1.41	0.52	0.92	0.37	0.65
5	1.76	0.65	1.15	0.37	0.65

Table (2): The objective focal properties for different values of a_2 under zero magnification condition at $NI / V_r^{1/2} = 30$.

a_2 mm	f_o mm	C_s mm	C_c mm	C_s/f_o	C_c/f_o
1	0.24	0.24	0.19	1.00	0.24
2	0.48	0.48	0.39	1.00	0.48
3	0.71	0.72	0.58	1.01	0.71
4	0.95	0.96	0.77	1.01	0.95
5	1.19	1.19	0.96	1.00	1.19

5. Conclusions

In the present work it was found the corresponding between the objective focal properties in the objective side under zero magnification condition with these properties in the image side under infinite magnification condition and vice versa .

The accuracy of the spline solution technique mainly depends on the spline interval width . However , as this width decrease the accuracy will increase and vice versa . This work can be extended further by using other models for asymmetrical axial magnetic fields.

References

- Al-Batat A.H. , Al- Nakeshli I.S. and Juma S.M. (2005) " Inverse design of asymmetrical magnetic lenses using a mathematical field model " Journal of the College of Education , Al- Mustansiriyah University " 5, 321-338 .
- Al-Obaidi H.N. (1995) " Determination of the design of magnetic electron lenses operated under reassigned magnification conditions " Ph.D.Thesis , University of Baghdad , Iraq .
- Al-Saadi S.R.A. (2007) " Improvement in applications of the theory of charged beam optics " Ph.D.Thesis , Al-Mustansiriyah University , Iraq .
- Grivet P. (1972) " Electron optics " Part 2nd ed. (Academic Press Ltd .Oxford) .
- Hawkes P.W (1982) " Magnetic electron lenses " (Springer- Verlag , Berlin) .
- Hawkes P.W. , and Kasper E. (1989) " Principle of electron optics " Vol.2 (Academic Press: London) .
- Juma S.M. , and Mulvey T. (1974) " New rotation free magnetic electron lenses " Vol.1.ed.J.Sanders and D.J. Good Child (Australian Academy of Sciences , Canberra) . 134 135 .
- Juma S.M. , and Mulvey T. (1978) " Miniature rotation free magnetic electron lenses for the electron microscopy " J.Phys.E: Sci.Inst. , 11,759-764 .
- Szilagyi M. (1988) " Electron and ion optics " (Plenum Press : New York) .
- Zhigarev A. (1975) " Electron optics and electron beam devices " (Mir . Publisher: Moscow) .